

Towards a Combined HERA Diffractive Deep Inelastic Scattering Measurement*

Paul Newman^a, Marta Ruspa^b

^a School of Physics & Astronomy, University of Birmingham, B15 2TT, UK.

^b Università del Piemonte Orientale, 28100 Novara, Italy.

Abstract

The diffractive dissociation of virtual photons, $\gamma^*p \rightarrow Xp$, has been studied with the H1 and ZEUS detectors at HERA using various complementary techniques. Events have been selected by direct tagging of the outgoing proton or by requiring a large rapidity gap between the proton and the system X . The diffractive contribution has also been unfolded by decomposition of the inclusive hadronic final state invariant mass distribution. Here, detailed comparisons are made between diffractive cross section measurements obtained from the different methods and the two experiments, showing them to be consistent within the large uncertainties associated with the treatment of proton dissociation processes. First steps are taken towards the combination of the H1 and ZEUS results.

1 Introduction

In the single diffractive dissociation process in proton-proton scattering, $pp \rightarrow Xp$, at least one of the beam hadrons emerges intact from the collision, having lost only a small fraction of its energy and gained only a small transverse momentum. In the analogous process involving virtual photons, $\gamma^*p \rightarrow Xp$ (figure 1) [2,3], an exchanged photon of virtuality Q^2 dissociates through its interaction with the proton at a squared four momentum transfer t to produce a hadronic system X with mass M_X . The fractional longitudinal momentum loss of the proton during the interaction is denoted $x_{\mathbb{P}}$, while the fraction of this momentum carried by the struck quark is denoted β . These variables are related to Bjorken x by $x = \beta x_{\mathbb{P}}$.

Diffractive interactions are often discussed in the framework of Regge phenomenology [4] in terms of the exchange of a ‘pomeron’ with vacuum quantum numbers. This interpretation in terms of a universal exchange is experimentally supported by the ‘proton vertex factorisation’, which holds to good approximation over much of the accessible kinematic range at low $x_{\mathbb{P}}$, whereby the dependences on variables describing the soft interaction with the proton ($x_{\mathbb{P}}, t$) factorise from those related to the hard interaction with the virtual photon (β, Q^2). Similar reactions, in which sub-leading Reggeon and pion trajectories are exchanged, have a negligible cross section at the smallest $x_{\mathbb{P}}$ values.

Significant progress has been made in understanding diffraction in terms of QCD by studying virtual photon dissociation in deep inelastic electron-proton (ep) scattering (diffractive DIS) at HERA. A recent review can be found at [5]. As well as being sensitive to novel features of parton dynamics in the high density, low x regime, diffractive DIS cross sections are used to extract diffractive parton density functions (DPDFs) [6–10], an essential ingredient in predicting many diffractive processes at the LHC and in estimating backgrounds to more exotic processes such as central exclusive Higgs production ($pp \rightarrow pHp$) [11].

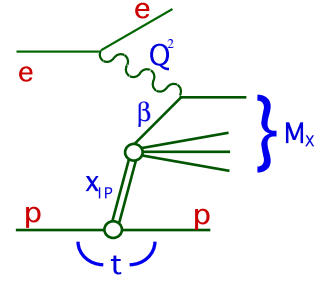


Fig. 1: Illustration of the kinematic variables describing the virtual photon dissociation process, $\gamma^*p \rightarrow Xp$, in ep collisions.

* Contributed to the Proceedings of the HERA-LHC Workshop [1].

Similarly to inclusive DIS, cross section measurements for the reaction $ep \rightarrow eXp$ are conventionally expressed in terms of the reduced diffractive cross section, $\sigma_r^{D(3)}$, which is related to the measured cross section by

$$\frac{d\sigma^{ep \rightarrow eXp}}{d\beta dQ^2 dx_{\mathbb{P}}} = \frac{4\pi\alpha^2}{\beta Q^4} \left[1 - y + \frac{y^2}{2} \right] \sigma_r^{D(3)}(\beta, Q^2, x_{\mathbb{P}}). \quad (1)$$

At moderate inelasticities y , $\sigma_r^{D(3)}$ corresponds to the diffractive structure function $F_2^{D(3)}$ to good approximation. In this contribution, we tackle the technical issue of compatibility between different $\sigma_r^{D(3)}$ data sets through detailed comparisons between different measurements by the H1 and ZEUS collaborations and take the first steps towards a combined HERA data set.

2 Methods of selecting diffraction at HERA

Experimentally, diffractive ep scattering is characterised by the presence of a leading proton in the final state retaining most of the initial state proton energy, and by a lack of hadronic activity in the forward (outgoing proton) direction, such that the system X is cleanly separated and M_X may be measured in the central detector components. These signatures have been widely exploited at HERA to select diffractive events by tagging the outgoing proton in the H1 Forward Proton Spectrometer or the ZEUS Leading Proton Spectrometer (proton-tagging method [7, 12–15]) or by requiring the presence of a large gap in the rapidity distribution of hadronic final state particles in the forward region (LRG method [6, 9, 16, 17]). In a third approach (M_X method [17–20]), the inclusive DIS sample is decomposed into diffractive and non-diffractive contributions based on their characteristic dependences on M_X .

The kinematic coverages of the LRG and M_X methods are limited to $x_{\mathbb{P}} \lesssim 0.05$ by the need to contain the system X in the central detector components. These two methods are equivalent for $M_X \rightarrow 0$, but differences are to be expected at larger M_X , where the LRG method measures the full cross section from all sources at a given $(x_{\mathbb{P}}, \beta, Q^2)$ point, whereas the M_X method involves the subtraction of a ‘non-diffractive’ component. LPS and FPS data extend to $x_{\mathbb{P}} \sim 0.1$ and are therefore the most sensitive to non-leading contributions, including Reggeon and pion trajectory exchanges. Apart from the proton dissociation treatment in the H1 case (see section 4.2), the cross sections measured by the proton-tagging and LRG methods are equivalent.

The methods differ substantially in their dominant sources of systematic uncertainty. In the LRG and M_X methods, the largest uncertainties arise from the admixture of low mass leading baryon systems other than protons. These include proton excitations to low mass states as well as leading neutrons produced via charge exchange reactions. All such contributions are collectively referred to here as ‘proton dissociation’, $ep \rightarrow eXN$, with the baryon state N having mass M_N . Proton dissociation processes cannot always be distinguished by the LRG and M_X methods from events in which the proton is scattered elastically. Conversely, low- $x_{\mathbb{P}}$ samples selected by the proton-tagging method have little or no proton dissociation background, but are subject to large uncertainties in the proton tagging efficiency, which is strongly dependent on the proton-beam optics. Proton spectrometers also allow a measurement of t , but the statistical precision is limited by their small acceptances.

Comparing the results from the three different methods is a powerful test of the control over the systematics of the measurements. At low $x_{\mathbb{P}}$, the ratio of results obtained by the LRG and M_X methods to those from the proton-tagging method can also be used to quantify the proton dissociation contributions in the former samples.

3 Data sets

A comprehensive comparison has been carried out between recent H1 and ZEUS measurements obtained with the three different methods. The data sets used are as follows.¹

- Three data sets collected with the ZEUS detector in the years 1999 and 2000. Overlapping samples have been analysed with the ZEUS Leading Proton Spectrometer (termed “**ZEUS LPS**”, based on a luminosity of 32.6 pb^{-1}) [16], with the LRG method (“**ZEUS LRG**”, 62.4 pb^{-1}) [16] and with the M_X method, relying on the Forward Plug Calorimeter (“**ZEUS FPC I**”, 4.2 pb^{-1} [19] and “**ZEUS FPC II**”, 63.4 pb^{-1} [20]).
- A set of data collected with the H1 Forward Proton Spectrometer (“**H1 FPS**”, 28.4 pb^{-1}) [15] in the years 1999 and 2000.
- A set of data collected with the H1 detector in the years 1997, 1999 and 2000 and analysed with the LRG method (“**H1 LRG**”, 2.0 pb^{-1} , 10.6 pb^{-1} and 61.6 pb^{-1} for small, intermediate and large Q^2 , respectively) [9].

The H1 LRG and FPS samples are statistically independent and are only weakly correlated through systematics. The three ZEUS samples also have different dominating systematics, but are not statistically independent. About 75% of events are common to both the ZEUS LRG and ZEUS FPC II data sets and 35% of the ZEUS LPS events are also contained in the ZEUS LRG sample.

4 Proton dissociation background and corrections

In proton dissociation processes at the lowest M_N , the dissociative system N often escapes entirely undetected into the forward beam-pipe. As M_N increases, it becomes more likely that dissociation products are detected in the instrumentation most sensitive to forward energy flow. The LRG and M_X methods therefore do not distinguish low M_N proton dissociation events from the case in which the proton is scattered elastically. Different cross-section definitions have been adopted, in which the proton dissociation contribution is either subtracted statistically, or else the quoted results are integrated over a specific range of M_N . Since understanding the proton dissociation contributions and the corresponding corrections is fundamental to comparisons between the different measurements, a detailed discussion is presented in the following.

In both the ZEUS LPS and the H1 FPS analyses, the contribution from proton dissociation events is negligible at small $x_{\text{IP}} \lesssim 0.02$. At the largest x_{IP} values, it becomes kinematically possible for the detected leading proton to be the result of a decay of an N^* or other proton excitation, the remaining decay products being unobserved. This background was estimated by ZEUS to contribute around 9% at $x_{\text{IP}} = 0.1$, using the PYTHIA Monte Carlo (MC) model [21]. In the H1 FPS analysis, using the RAPGAP [22] implementation of the DIFFVM proton dissociation model [23], it was estimated to reach 3% at $x_{\text{IP}} = 0.08$.

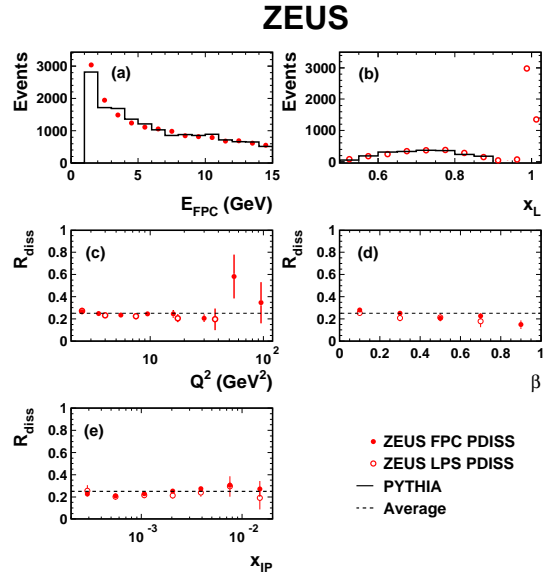


Fig. 2: (a) FPC energy and (b) LPS x_L distributions for ZEUS proton dissociation samples (see text), with data compared to the tuned PYTHIA model. (c-e) Extracted fractions of proton dissociation events in the ZEUS LRG sample as a function of Q^2 , β and x_{IP} after integration over the other variables [16].

¹The comparisons here are restricted to published data and do not yet include the precise H1 LRG and M_X method results obtained from 1999-2004 running [17].

Proton dissociation contributions in the LRG and M_X methods can be controlled using dedicated proton dissociation simulations tuned in M_N regions where dissociating protons leave signals in the detectors, and extrapolated into the M_N regions where the dissociation products are typically not detected. In addition to this procedure, both H1 and ZEUS use standard simulations of non-diffractive processes to control the small migrations of very high M_N or $x_{\mathbb{P}}$ events into the measurement region, which occur due to inefficiencies of the forward detectors.

4.1 ZEUS LRG

In the recent ZEUS analysis, the PYTHIA simulation was tuned to proton dissociation signals. Two samples were selected by requiring activity either in the forward plug calorimeter (FPC) or at relatively low proton energy in the LPS. The samples thus include the low M_N region in which proton dissociation products are invisible to the central detector. The generated distributions were reweighted in M_N , M_X and Q^2 to best describe the energy distribution in the FPC (E_{FPC}), and the scattered proton energy fraction distribution (x_L) in the LPS. Figures 2a and 2b show the comparison of the reweighted PYTHIA model with the two proton dissociation samples as a function of these variables. Also shown in figures 2c-e is the resulting estimate of the fraction of proton dissociation events in the LRG sample as a function of Q^2 , β and $x_{\mathbb{P}}$. This fraction, obtained separately from the FPC and LPS samples, is constant at the level of 25%.

The ratios of cross sections extracted from the ZEUS LPS and LRG data (the latter uncorrected for proton dissociation background), are shown in figure 3. There is no significant dependence on Q^2 , $x_{\mathbb{P}}$ or β , illustrating the low $x_{\mathbb{P}}$ compatibility between the two methods. The ratio averages to $0.76 \pm 0.01(\text{stat.})_{-0.02}^{+0.03}(\text{syst.})_{-0.05}^{+0.08}(\text{norm.})$, the last error reflecting the normalisation uncertainty of the LPS data. The proton dissociation background fraction in the LRG data is thus $24 \pm 1(\text{stat.})_{-3}^{+2}(\text{syst.})_{-8}^{+5}(\text{norm.})\%$, in agreement with the result of the MC study, $25 \pm 1(\text{stat.}) \pm 3(\text{syst.})\%$ (figure 2). Unless stated otherwise, the ZEUS LRG data are corrected by this factor in the following and thus correspond exclusively to the truly proton-elastic process.

4.2 H1 LRG

The contribution from proton dissociation in the H1 LRG analysis is constrained through the DIFFVM MC [23] model, normalised using the response to large M_N events leaving signals in the forward and central detector components [9, 24].

The data are corrected using DIFFVM to $M_N < 1.6$ GeV. The H1 LRG data are then compared with the H1 FPS measurement, in order to extract the proton dissociation cross section with $M_N < 1.6$ GeV directly from the data. The ratio of the two measurements, after projection onto the Q^2 , $x_{\mathbb{P}}$ and β axes, is shown in figure 4. There is no evidence for any dependence on any of the kinematic variables. as expected in the framework of proton vertex factorisation. The average value of the ratio is $1.23 \pm 0.03(\text{stat.}) \pm 0.16(\text{syst.})$, the largest uncertainty arising from the FPS efficiency. The result

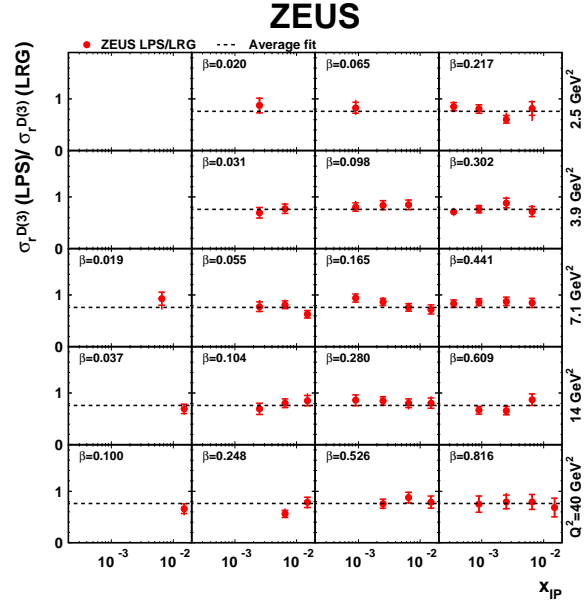


Fig. 3: The ratio of the ZEUS LPS measurement ($M_N = m_p$) to the ZEUS LRG measurement before subtraction of proton dissociation background [16]. The lines represent the average value of this ratio. An overall normalisation uncertainty of $_{-8}^{+11}\%$ is not included in the errors shown.

is in good agreement with the DIFFVM estimate of $1.15^{+0.15}_{-0.08}$. The data and DIFFVM ratios translate into proton dissociation background fractions of 19 % and 13 %, respectively, consistent within the uncertainties. The similarity between the proton dissociation fractions in the raw H1 and ZEUS LRG selections is to be expected given the similar forward detector acceptances of the two experiments.

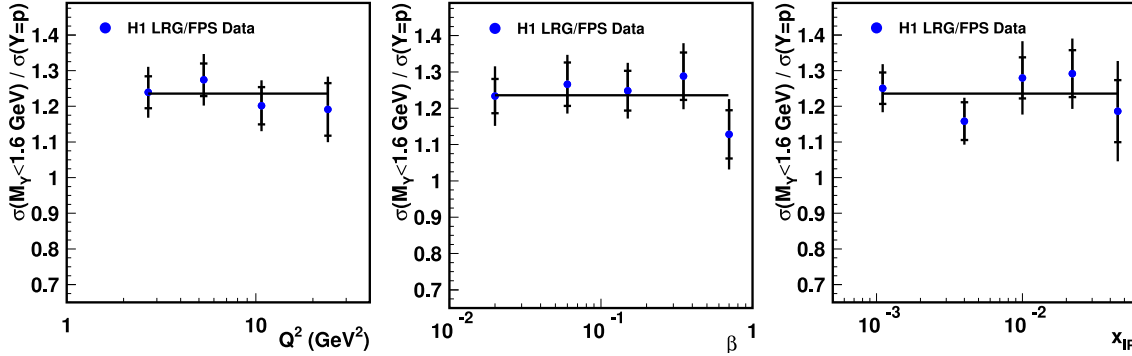


Fig. 4: The ratio of the H1 LRG measurement (corrected to $M_N < 1.6$ GeV) to the H1 FPS measurement ($M_N = m_p$), after integration over the variables not shown in each case [15]. The lines represent a fit to the data assuming no dependence on any of the variables. An overall normalisation uncertainty of 13% is not included in the errors shown.

4.3 ZEUS FPC

The proton dissociation treatment is also critical in the M_X method, where the diffractive contribution is separated from the non-diffractive component in a fit to the inclusive $\ln M_X^2$ distribution. Proton dissociation events with sufficiently large M_N for dissociation products to reach the FPC and central detectors lead to a reconstructed M_X value which is larger than the actual photon dissociation mass. The resulting distortion of the $\ln M_X^2$ distribution affects the diffractive contribution extracted in the fit if corrections are not made. According to the SANG MC model, the N system contaminates the M_X reconstruction for $M_N > 2.3$ GeV on average [25], and events in this M_N range are therefore subtracted using SANG before the $\ln M_X^2$ distribution is decomposed. The upper M_N cut in the SANG sample is defined by $(M_N/W)^2 < 0.1$, which leads to a variation of the subtracted fraction of events with W , the centre-of-mass energy of the photon-proton system. This contrasts with the LRG method, where MC studies confirm that the rapidity gap requirement efficiently eliminates proton dissociation at large M_N , the remaining fractional low M_N contribution being independent of kinematics to good approximation (figures 3 and 4).

Despite these difficulties, there is acceptable agreement between the ZEUS FPC data and the ZEUS LRG measurement. A global fit comparing the normalisations of the two data sets (after correcting the LRG data to $M_N = m_p$) yields a normalisation factor of 0.83 ± 0.04 to be applied to the ZEUS FPC results. This factor is compatible with expectations for the residual proton dissociation contribution based on the MC studies in sections 4.1 and 4.2.

5 Cross section comparisons

Due to their differing M_N coverages, the $\sigma_r^{D(3)}$ measurements from the different data sets are not directly comparable. However, assuming the factorisation of the M_N dependence which is suggested in the data, varying the M_N range should introduce only global normalisation differences, which can be estimated using the proton dissociation simulations.

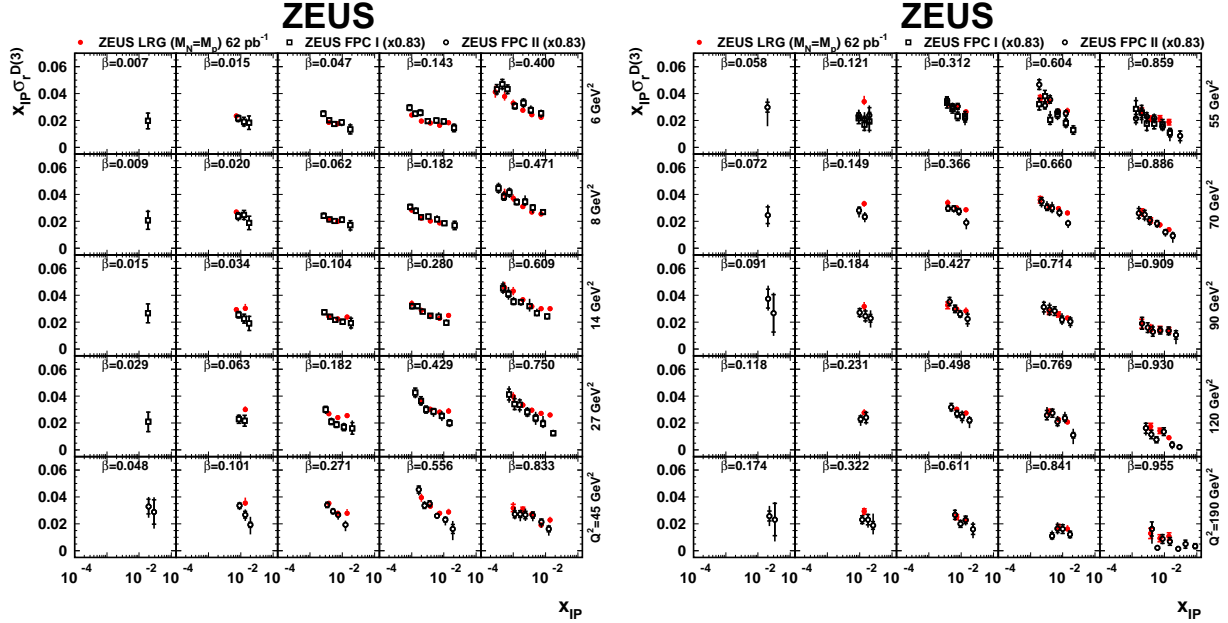


Fig. 5: Comparison between the ZEUS M_X method ('FPC I' and 'FPC II') and ZEUS LRG method data [16]. As explained in the text, the M_X method data are scaled by a constant factor of 0.83 to account for proton dissociation contributions with $M_N < 2.3$ GeV.

5.1 Comparison between LRG and M_X methods

ZEUS cross section measurements obtained with the LRG and M_X methods are compared in figure 5. The LRG data are corrected to $M_N = M_p$ as described in section 4.1 and the relative normalisation factor of 0.83 (section 4.3) is applied to the ZEUS FPC data to account for residual proton dissociation. The overall agreement between the two measurements is good, apart from some differences at large $x_{\text{IP}} \gtrsim 0.01$. The Q^2 dependence of the M_X method data is also slightly weaker than that of the LRG data.

5.2 Comparison between ZEUS LPS and H1 FPS measurements

The ZEUS LPS and H1 FPS data are compared in figure 6. For this comparison, the ZEUS results are extracted at the same β and Q^2 values as H1 and are therefore not affected by extrapolation uncertainties. The shape agreement is satisfactory and the overall normalisation discrepancy of around 10% lies within the large combined normalisation uncertainty of around 14%.

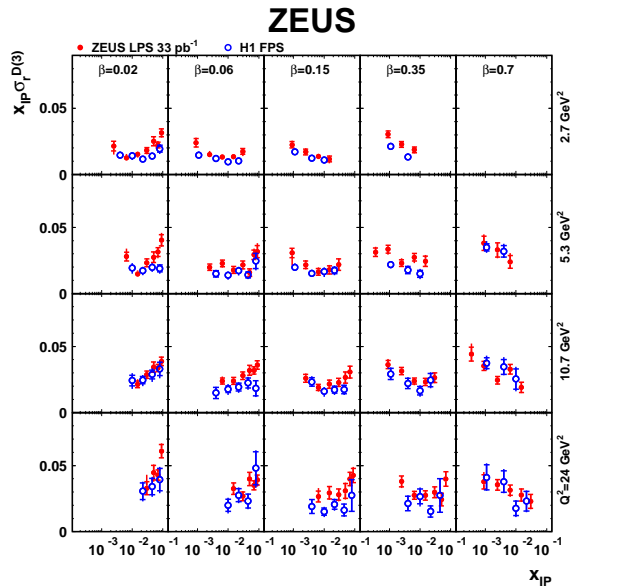


Fig. 6: Comparison between ZEUS LPS and H1 FPS measurements [16]. Normalisation uncertainties of $\pm 10\%$ (H1) and $+11\%$ (ZEUS) are not shown.

5.3 Comparison between ZEUS and H1 LRG measurements

The ZEUS LRG data are extracted at the H1 β and $x_{\mathbb{P}}$ values, but at different Q^2 values. In order to match the $M_N < 1.6$ GeV range of the H1 data, a global factor of 0.91 ± 0.07 , estimated with PYTHIA, is applied to the ZEUS LRG data in place of the correction to an elastic proton cross section. After this procedure, the ZEUS data remain higher than those of H1 by 13% on average, as estimated with a global fit comparing the normalisations of the two data sets for $Q^2 > 6$ GeV². This normalisation discrepancy is similar to that between the H1 FPS and the ZEUS LPS data sets. It is in line with the errors due to the 8% uncertainty on the proton dissociation correction in the ZEUS LRG data and the 7% combined relative normalisation uncertainty between the two LRG data sets.

In figure 7, the ZEUS results are scaled by a factor 0.91×0.87 (the factor $0.87 = 1 - 0.13$ normalising the ZEUS to the H1 data) and compared with the H1 LRG measurement. An excellent agreement between the Q^2 dependences is revealed throughout most of the phase space. There are small deviations between the β dependences of the two measurements at the highest and lowest β values. The results of the ‘H1 Fit B’ NLO QCD DPDF fit to the H1 LRG data [9] is also shown. It gives a good description of the data at large Q^2 . However, the extrapolation beyond the fitted region ($Q^2 \geq 8.5$ GeV²) undershoots the precise new ZEUS low Q^2 LRG data, confirming the observation in [9] that a standard DGLAP fit to the lowest Q^2 data is problematic.

6 A First Combination of Data Sets

For easy future consumption at the LHC and elsewhere, it is desirable to combine the various H1 and ZEUS diffractive DIS measurements into a single easily digestible HERA data set. Here we take the first steps towards this goal, by making a simple error-weighted average of the H1 and ZEUS LRG data sets, ignoring correlations between the data points due to the systematic errors. LPS and M_X method data are not considered at this stage. For the purpose of this exercise, the ZEUS normalisation is fixed to that of H1 as described in section 5.3 and shown in figure 7. The normalisation of the combined data thus has an uncertainty beyond the 10% level. Combinations can only meaningfully be made where there is basic agreement between the different measurements. Since this is not always the case at the lowest $x_{\mathbb{P}}$ values, we restrict the averaging to the $x_{\mathbb{P}} = 0.003$ and $x_{\mathbb{P}} = 0.01$ data. The combinations are performed throughout the measured Q^2 range, including the $Q^2 < 8.5$ GeV² region, beyond the range of the ‘H1 Fit B’ parameterisation which is compared with the data.

To account for the differences between the Q^2 binning choices, H1 data points are adjusted to the ZEUS Q^2 values by applying small correction factors calculated using the ‘H1 Fit B’ parameterisation. Where both collaborations then have measurements at a given $(Q^2, x_{\mathbb{P}}, \beta)$ point, a simple weighted average is taken, using the quadratic sum of statistical and systematic uncertainties for each experiment, excluding normalisation uncertainties. At $(Q^2, x_{\mathbb{P}}, \beta)$ points where only one experiment has a measurement, that result is carried directly into the combined data set.

The results of this averaging procedure² are shown in figure 8. They are indicative of the sort of precision which is achievable through combinations, with many data points having errors at the 3 – 4% level, excluding the normalisation uncertainty. At $x_{\mathbb{P}} = 0.01$ the combined data agree well with the ‘H1 Fit B’ DPDF parameterisation in its region of validity. At $x_{\mathbb{P}} = 0.003$ the Q^2 dependences are also in good agreement with the parameterisation in the β and Q^2 region of the fit, with the exception of the highest β value, where the average is pulled towards the more precise ZEUS data.

More sophisticated averaging methods may be used in the future, for example that [26] developed to perform similar combinations of inclusive HERA data, with a full systematic error treatment. No attempt has yet been made to extract DPDFs from the combined data. Based on the combined $\sigma_r^{D(3)}$ and its Q^2 dependence shown here, no significant conflict is expected with the quark or gluon densities of existing DPDF sets such as ‘H1 Fit B’ in the bulk of the phase space. However, small modifications are

²The authors take full responsibility for this combined data set; it is not an official H1/ZEUS result.

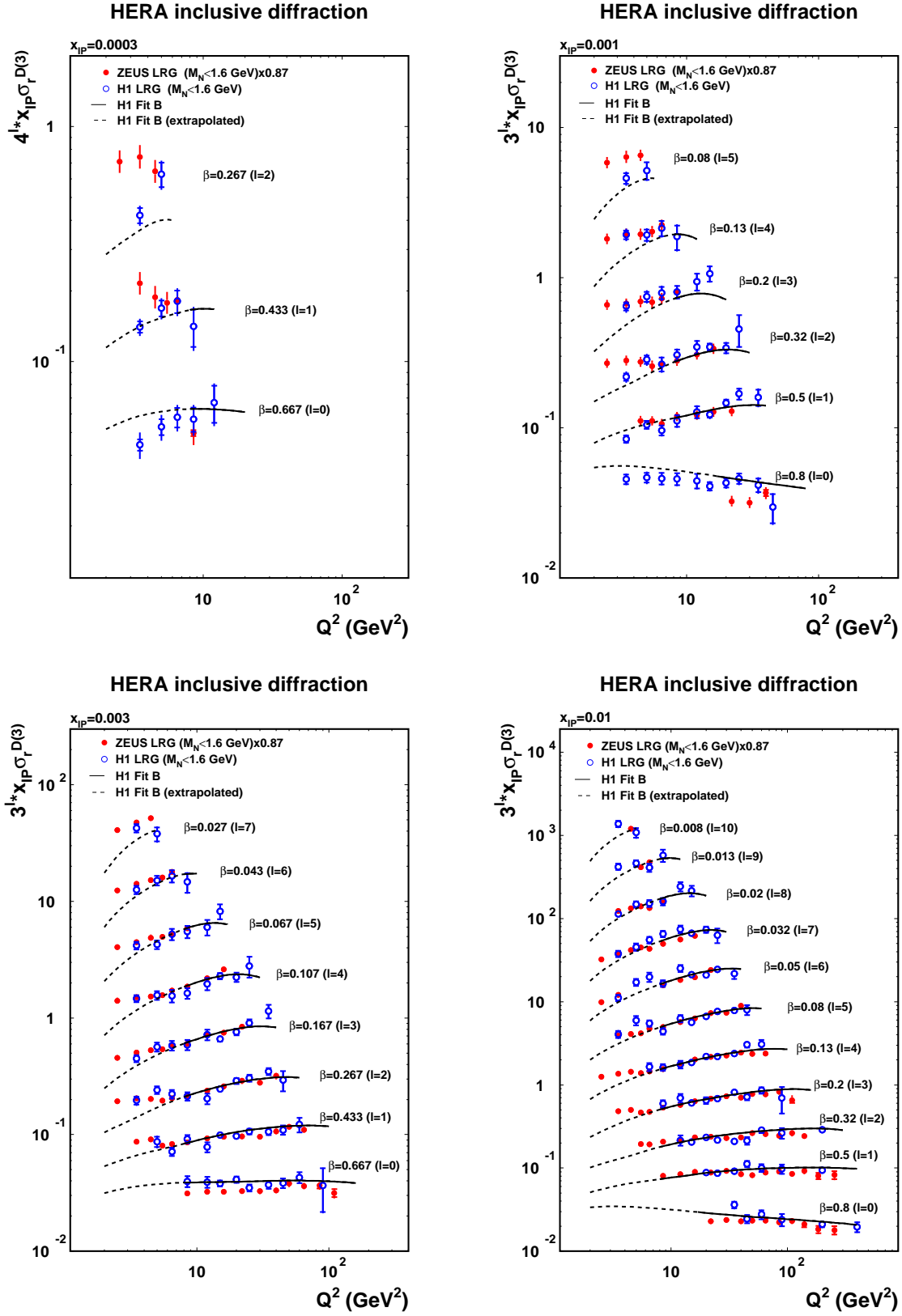


Fig. 7: Comparison between the H1 and ZEUS LRG measurements after correcting both data sets to $M_N < 1.6$ GeV and applying a further scale factor of 0.87 (corresponding to the average normalisation difference) to the ZEUS data. The measurements are compared with the results of the 'H1 Fit B' DPDF extraction, which was based on the H1 data shown. Further H1 data at $x_{IP} = 0.03$ are not shown.

likely to be necessary to the quark densities at small and large β values and understanding the region $Q^2 \lesssim 8.5 \text{ GeV}^2$ remains a challenge.

7 Summary

H1 and ZEUS diffractive DIS data obtained by various methods with very different systematics have been compared in detail. All measurements are broadly consistent in the shapes of the distributions. The comparisons between proton tagging and LRG method data internally to the two collaborations give compatible results on the proton dissociation contributions in the raw LRG selections. There is a global normalisation difference at the 13% level between the LRG measurements of the two experiments, which is a little beyond one standard deviation in the combined normalisation uncertainty. A similar difference is visible between the normalisations of the H1 and ZEUS proton tagged data.

A first step has been taken towards combining the two sets of LRG data, by arbitrarily fixing the normalisation to that of the H1 data set and ignoring correlations within the systematic uncertainties in obtaining weighted averages. The results hint at the precision which might be obtained in the future with a more complete procedure.

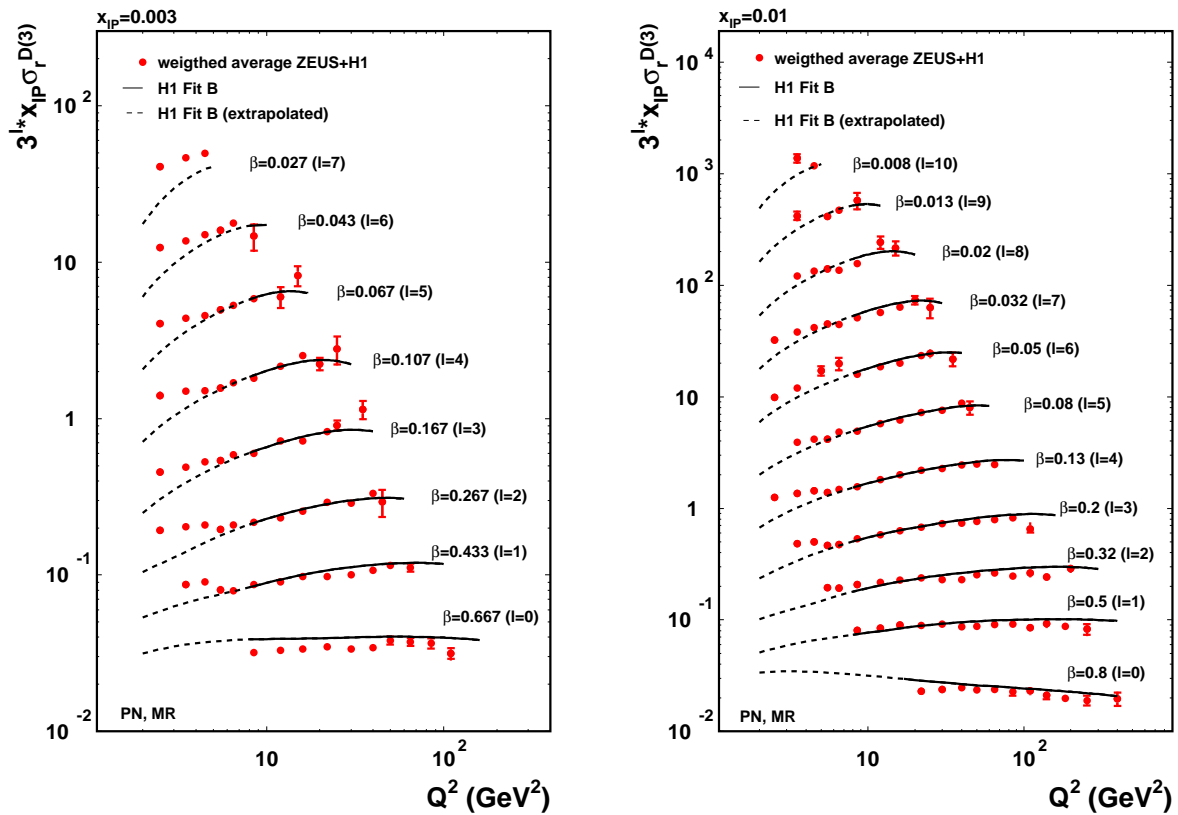


Fig. 8: Combination of the H1 and ZEUS LRG data following the procedure described in the text. The global normalisation is fixed to that of the H1 measurement, in order most easily to compare the data with the 'H1 Fit B' DPDF results.

References

- [1] Proceedings of the 2nd, 3rd and 4th HERA-LHC Workshops, in litt., eds. de Roeck, Jung (2009); <http://www.desy.de/~heralhc/>.
- [2] ZEUS Collaboration, M. Derrick et al., Phys. Lett. **B 315**, 481 (1993).
- [3] H1 Collaboration, T. Ahmed et al., Nucl. Phys. **B 429**, 477 (1994).
- [4] P.D.B. Collins, *An Introduction to Regge Theory and High Energy Physics*. Cambridge University Press, Cambridge, 1977.
- [5] M. Arneodo and M. Diehl, Proceedings of the 1st HERA-LHC Workshop, eds. de Roeck, Jung, CERN-2005-014, hep-ph/0511047.
- [6] H1 Collaboration, C. Adloff et al., Z. Phys. **C 76**, 613 (1997).
- [7] ZEUS Collaboration, S. Chekanov et al., Eur. Phys. J. **C 38**, 43 (2004).
- [8] A. Martin, M. Ryskin, G. Watt, Eur. Phys. J. **C 44**, 69 (2005).
- [9] H1 Collaboration, A. Aktas et al., Eur. Phys. J. **C 48**, 715 (2006).
- [10] H1 Collaboration, A. Aktas et al., JHEP 0710:042 (2007).
- [11] FP420 R&D Collaboration, hep-ex/0806.0302 (2008).
- [12] ZEUS Collaboration, J. Breitweg et al., Eur. Phys. J. **C 1**, 81 (1997).
- [13] H1 Collaboration, C. Adloff et al., Eur. Phys. J. **C 6**, 587 (1999).
- [14] ZEUS Collaboration, S. Chekanov et al., Eur. Phys. J. **C 25**, 169 (2002).
- [15] H1 Collaboration, A. Aktas et al., Eur. Phys. J. **C 48**, 749 (2006).
- [16] ZEUS Collaboration, S. Chekanov et al., DESY 08-175, submitted to Nucl. Phys. **B**.
- [17] H1 Collaboration, H1prelim-06-014 (presented at DIS2006, E. Sauvan).
- [18] ZEUS Collaboration, S. Chekanov et al., Eur. Phys. J. **C 25**, 69 (2002).
- [19] ZEUS Collaboration, S. Chekanov et al., Nucl. Phys. **B 713**, 3 (2005).
- [20] ZEUS Collaboration, S. Chekanov et al., Nucl. Phys. **B 800**, 1 (2008).
- [21] T. Sjöstrand, L. Lönnblad and S. Mrenna, hep-ph/0108264 (2001).
- [22] H. Jung, Comput. Phys. Commun. **86**, 147 (1995).
- [23] B. List and A. Mastroberardino, Proceedings of the Workshop on MC Generators for HERA Physics, p. 396 (1999).
- [24] C. Johnson, *Ph.D. Thesis, University of Birmingham*. 2002.
- [25] H. Lim, *Ph.D. Thesis, The Graduate School, Kyungpook National University, Taegu (Republic of Korea)*. Unpublished, 2002.
- [26] A. Glazov, Proceedings of DIS 2005, Madison, USA, eds Smith, Dasu, (AIP 2005).